Taylor & Francis
Taylor & Francis Group

Particulate Science and Technology

An International Journal

ISSN: (Print) (Online) Journal homepage: www.tandfonline.com/journals/upst20

A distinctive determination of circular nozzles in downcomer for column flotation

Hüseyin Vapur, Soner Top & Mahmut Altiner

To cite this article: Hüseyin Vapur, Soner Top & Mahmut Altiner (2023) A distinctive determination of circular nozzles in downcomer for column flotation, Particulate Science and Technology, 41:7, 1015-1022, DOI: 10.1080/02726351.2023.2164878

To link to this article: https://doi.org/10.1080/02726351.2023.2164878

PARTICULATE SCIENCE AND TECHNOLOGY
2023, VOL. 41, NO. 7, 1015–1022
https://doi.org/10.1080/02726351.2023.2164878

A distinctive determination of circular nozzles in downcomer for column flotation

Hüseyin Vapur[a], Soner Top[b], and Mahmut Altiner[a]

[a]Mining Engineering Department, Cukurova University, Adana, Turkey; [b]Nanotechnology Engineering Department, Abdullah Gül University, Kayseri, Turkey

ABSTRACT

This study aims to recover clean coal from valuable hard coal tailings (HCT), which have been used as solid fuels in a thermal power plant, through convenient conditions. The effective diameters of circular nozzles on the recovery of HCT were investigated by using the Jameson cell (JC) as the main purpose. Preliminary tests were conducted to determine the type and dosages of the collector and frother. The JC test results were evaluated by Yates and Box Behnken based on ANOVA analysis, statistically. It was observed that 3,000 g/ton of diesel oil, 300 g/ton of MIBC, 100 g/ton of Na_2SiO_3, and 60 cm of downcomer depth were found applicable levels of parameters. The decrease of the diameter increased the venturi effect of downcomer which provided the best recovery ratio of 97.79%. Besides, the results of kinetic models were obtained with desired efficiencies ($CR_\infty = 94.77\%$, $k_{coal} = 1.20$, $R^2 = 0.98$ and SI = 2.40). The best diameter was 5 cm supplied a short time and high carrying capacity (CC) for concentrate.

KEYWORDS

Coking coal tailings; Jameson cell; downcomer; circular nozzle; carrying capacity

1. Introduction

The statistics indicate that the top 10 coal-producing countries have access to more than 30 billion metric tons of coal owing to the problems involved in the recovery of coal fines. These coal fines are either added to steam coal or left on stockpiles and slurry ponds close to mining sites (G. Wang et al. 2018; Ramudzwagi et al. 2020). Annually, the total amount of bituminous coal as slime used in thermal power plants is nearly 0.5 million tonnes in Turkey (Hacifazlioglu and Toroglu, 2007). The flotation method is applied in the enrichment of very fine coals with rising amounts due to the increasing mechanized excavation methods in coal mining (Barraza, Guerrero, and Pineres 2013; Meshram et al. 2015; Ni et al. 2018). This method is widely used in the enrichment of fine coals due to their hydrophobic nature, depending on directly proportional to the age of the coals (Y. Li et al. 2019). Besides, there are new flotation methods such as column flotation (J. Wang and Wang 2018; Dey, Paul, and Pani 2013), micro-bubble flotation (B. Li et al. 2003; Xing et al. 2017), Jameson flotation (Vapur, Bayat, and Ucurum 2010; Zhu et al. 2018). The interaction of fine minerals and bubbles takes place in the downcomer, which is a vertical pipe, an essential part of this technology. The pulp forms a liquid jet in this pipe. The possibility of a collision between the bubbles and mineral particles is high because the device produces small air bubbles and a high-density air bubble in the downcomer (G. Wang et al. 2018). The JC method has high CC due to the short time of residence in the device (Harbort et al. 2003; Yan and Jameson 2004; You et al. 2017).

In this study, new types of circular (hemispherical) nozzles were used in JC tests. The goals here were to increase the dowcomer outlet diameter, reduce turbulence and increase recovery. As a biased approach, the use of circular nozzles has always been effective in industrial applications such as water jets, fire extinguishing nozzles, etc. Preliminary kinetic model was developed for Denver flotation using Yates test design. The test results of the modified JC were modeled with the design of experiment (Box Behnken). The usage of innovative types of circular nozzles in JC were examined as an effective approach.

2. Materials and methods

In this study, the fines of HTC supplied from Catalağzı Thermal Power Plant located in Turkey were used in recovery tests. The bulk sample was obtained by dewatering fine-sized coal (−0.5 µm) which was a mixture of the intermediate products obtained from gravitational methods such as jig, float-sink, etc. (Table 1). The total sulfur and fixed carbon of the sample were determined using an Eltra Cs 580 Carbon Sulfur Determinator. XRF (X-ray fluorescence) analysis was applied to the ash of the sample in order to determine inorganic compounds as % values (SiO_2: 24.17, Al_2O_3: 13.78, Fe_2O_3: 4.90, CaO: 2.69, K_2O: 2.32, TiO_2: 0.86, BaO: 0.36, V_2O_5: 0.06, and the others: 1.83).

CONTACT Hüseyin Vapur hvapur@cu.edu.tr Mining Engineering Department, Cukurova University, Adana, Turkey.

The XRD peaks of the sample ash mainly consist of quartz (SiO_2) and mullite ($3Al_2O_3.2SiO_2$) as the major hydrophilic minerals. Besides, magnetite (Fe_3O_4), calcium oxide (CaO) and kaolinite ($Al_2Si_2O_5(OH)_4$) are minor minerals in the ashes (Figure 1).

The sample was firstly crushed below 1.0 mm using a lab-scale jaw crusher and then ground with a ball mill under the dry condition. The optimum grinding time was found to be 10 min. (d_{80}: 130 µm) according to Figure 2. The milling conditions were as follows: 9 kg balls (4.5 cm, 3 cm and 2 cm in diameter), 500 g sample, and 70 rpm speed as 70% of the critical speed.

The combustible recovery (CR%), ash recovery (AR%) and ash removal (R%) values were calculated using the following equations (R% = 1 − AR%). Where C is the mass of the floating materials (g), c is the ash content of the floating materials (%), F is the mass of the feeding samples, and f is the ash content of the feeding samples (%).

$$\left(CR\% = \frac{C(100-c)}{F(100-f)} \times 100\right) \quad (1)$$

$$AR\% = \left(\frac{Cxc}{Fxf} \times 100\right) \quad (2)$$

Preliminary tests were carried out with Denver cell to select a frother (MIBC-Methyl isobutyl carbinol and pine oil as popular reagents) and a nonionic collector (kerosene and diesel oil). The volume of cell was 1 L and the conditioning time was 5 min. Then, the air valve was opened and floated concentrate was collected for 6 min. A full factorial test design with 2^3 (Yates-ANOVA) was used to select the optimum solid/water ratio by weight (10% and 30%). The main parameters were reagent dosage, flotation time, solid ratio, and airflow rate. In the Yates tests, variables were selected as follows: X_1: stirring speed (rpm), X_2: collector (g/ton), X_3: frother (g/ton) (Table 2). The stable parameters for tests were pH: 6.5–7, and d_{80}: 130 µm.

2.1. Jameson cell tests with semi-circular nozzles

A modified JC depicted in Figure 3 was redesigned to determine a convenient diameter of circular nozzles with Box Behnken tests for five types (d_1:5 mm, d_2:7 mm, d_3:9 mm, d_4:11 mm, d_5:13 mm) (Figure 4). The Jameson flotation test apparatus comprises three main parts: a conditioning tank, pump for pulp circulation and Jameson cell, which divided into two main parts: Jameson cell (10 cm in diameter and 75 cm in length) and downcomer (2 cm in diameter and

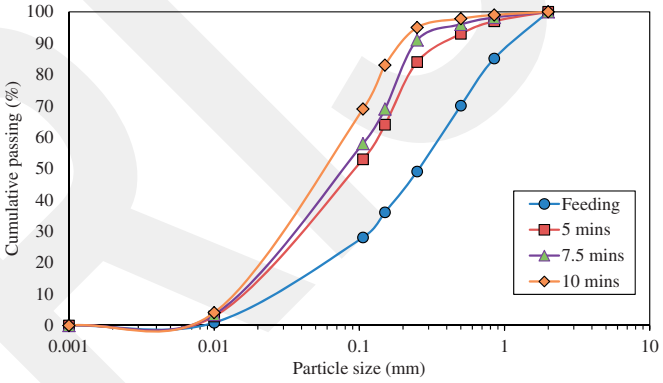

Figure 2. Particle size analysis for optimum grinding conditions of the sample.

Table 1. Basic analysis of the HCT sample.

Contents	%
Moisture	1.39
Ash	46.78
Volatile matter	18.52
Total sulfur	0.38
Calorific value (kcal/kg) ± 100	4,244
Fixed carbon	33.38

Table 2. The base levels of Yates design for ANOVA.

Parameter	Low level	Base level	High level
A = Stirring speed (rpm)	1,300	1,400	1,500
B = Collector dosage (g/ton)	1,125	2,250	3,375
C = Frother dosage (g/ton)	112.5	225	337.5

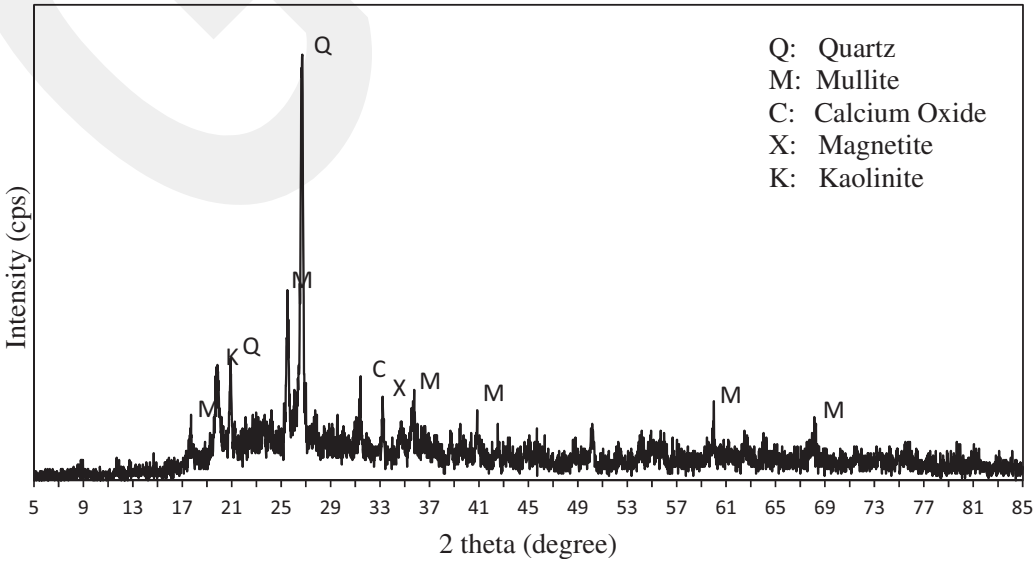

Figure 1. XRD pattern and main minerals for the ignited ash.

100 cm in length). The pulp was circulated via the pump and controlled with valves. Then, the pulp was left from the condition tank and went into the Jameson cell, in which fine particles were contacted with air and a washwater was used for removing impurities from surfaces of the froths. The vacuumed air was provided by the venturi effect of the downcomer.

The average CC of the test column was 25 ± 0.43 L/min. The bias factor (BF) is one of the most important characteristics of flotation columns and is described as the net water stream percolating downward from the froth or the corresponding net water flow difference between the tailings and feed streams. This factor, indicating whether there are froth zones or not, is calculated using Equation (3) suggested by Mohanty and Honaker (1999). Where Q_T is the flow rate of tailing (4.05 L/min), Q_F is the flow rate of feed (3.15 L/min), and Q_{WW} is the flow rate of wash water (3.0 L/min). The liquid loading rate (L) was calculated as 0.515 m^3/m^2.min from the relationship with column diameter using Equation (4) (Coker 1991). It depends on the CC and flow rate. Where D is column diameter (0.1 m) and Q_F is the flow rate (4.05 L/min). The increase in the bias factor makes it difficult to climb the particles in the froth zone, reducing the yield% and increasing the grade%. Negative bias prevents froth formation as a general rule. In this study, the optimum positive bias value (0.3 ± 0.05) was used for further optimization as a constant parameter. In the Box Behnken tests, variables were selected as follows: X_1: collector (g/ton), X_2: frother (g/ton), X_3: downcomer height (cm). The constant parameters were pH: 6.5–7, d_{80}: 200 µm (particle size was rearranged to reduce grinding costs, minimize the amount of material down to slime size, and increase industrial applicability), conditioning time: 4 min, flotation time: 7 min, Na_2SiO_3 depressant: 100 g/ton, and solid/water ratio: 10%.

$$BF = (Q_T - Q_F)/Q_{WW} \quad (3)$$

$$L = 4Q_{F/\pi}D^2 \quad (4)$$

The first-order kinetic model, which was broadly accepted by researchers for the flotation method, was used to reveal process utilization (Wills and Finch 2015; Asghar, Ahmad, and Behnam 2015). The kinetic models were derived from the following calculations. The equation $\int_{Co}^{C}\frac{dc}{C} = -k\int_{to}^{t} dt$ can be rewritten as $Ln\frac{C}{Co} = -kt$. In terms of conversion, the rate equation becomes $= 1 - e^{-kt}$. In the experiments performed with the redesigned JC with modified first-order kinetic model in Equation (5), which was proposed for use in flotation studies by Wills and Finch (2015), were applied using 500 g of HCT fines.

The first-order kinetic model:

$$(CR = CR_\infty(1 - e^{-kt})), \quad (5)$$

where CR (%) is the recovery at t times (min), CR_∞ is the ultimate yield or recovery (%), and k is the rate constant.

The chance of the fine particles colliding with the bubbles depends on the amount of fine bubbles in the cell. The lack of fine bubbles leads to low recovery in flotation (Ahmed and Jameson 1985; Miettinen, Ralston, and Fornasiero 2010). In the light of the experimental conditions, the bubble sizes ranged from 0.5 to 1 mm in the modified JC and these values were observed to be between 0.5 and 2 mm in the conventional Denver cell. The bubble sizes were found to be similar to previous studies (Gürsoy and Öteyaka 2015; Mazahernasab and Ahmadi 2016; Sahbaz and Demir 2020).

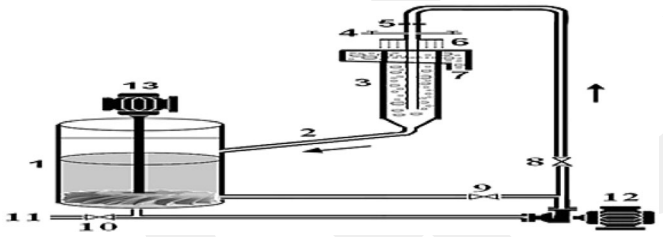

Figure 3. Schematic view of the modified Jameson flotation machine: conditioning (1), cycling of pulp (2), cell (3), air inlet (4), assembly of semi-circle nozzles (5), wash water (6), concentrate (7), valves (8–10), discharge (11), pumps (12–13).

3. Results and discussion

Firstly, the experiments were conducted using diesel oil and kerosene for collector selection with pine oil as frother. Each experiment was repeated 4 times and the results are given in Table 3. Close yield values were found and the diesel oil was selected due to economic reasons (with 91.62% CR). Then pine oil was compared with MIBC for the selection of frother and MIBC was found as an optimum frother (with

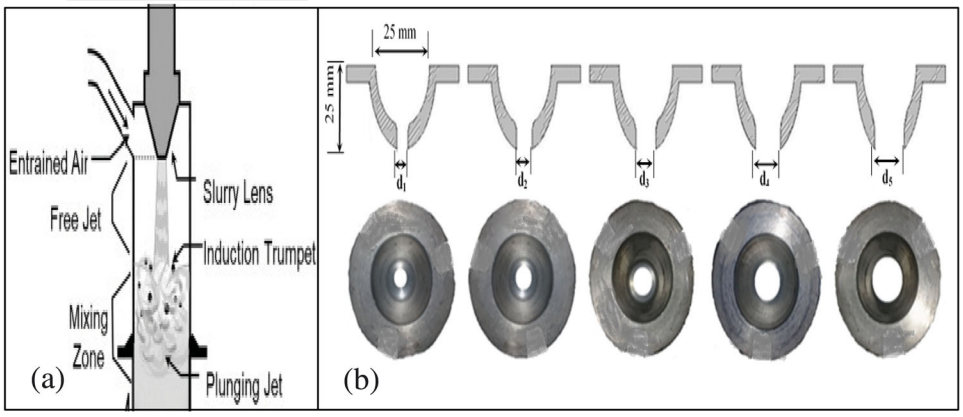

Figure 4. (a) The downcomer and (b) the semi-circular nozzles made of brass alloy (front-section views and overviews).

94.14% CR). The experimental conditions were as follows; solid/water ratio: 20%, pine oil: 100 g/t, pH: 6.5–7.0, collector: 1,000 g/ton, condition time: 5 min, flotation time: 5 min., stirring speed: 1,400 rpm, sample weight: 250 g, and d_{80}: 0.13 mm.

Yates test conditions are seen in Table 4. In the classical flotation tests, solid/water ratio of 10% have better results than others as CR values. The highest CR was obtained as 96.91% for the c-coded test with 10% solid ratio, and the average yield was 90.36% (Figure 5). The average CR at 20% solid/water ratio was 92.74% with ±3.03 variance. However, the highest CR was 91.32% for the c-coded tests and the average CR was 85.92%. In the experiments conducted with the Yates technique, an average yield of 85.90% was achieved at a 30% solid/water ratio. The kinetic models obtained at the optimum test conditions for 10% and 30% solids are given in Figure 6.

The flotation times were shorter due to using a low amount of sample in the Denver cell (110 g). The solid/water ratio of 10% was found to be appropriate in terms of CRs. Obtained ANOVA model of Yates design at 10% solid/water ratio for CR was given as follows:

$$Y = 90.36 - 2.24X_1X_2 - 1.44X_3 - 3.37\ X_1X_3 - 4.49X_2X_3 \quad (6)$$

Where X_n values are encoded. The coefficients in the function were found by dividing the values in the total effect column by the total number of experiments. Predicted values in Table 4 were calculated according to Equation 6.

In the similar research of Hacifazlioglu and Toroglu (2007), three types of nozzles which were classic, five hole and double crescent moon were used. There was one size for each nozzle and the technical sizes of the holes were not given, fully. Besides, time dependent kinetic modeling was not given, too. The percentage of solids were 4% and 10%. In addition, the circular nozzle was flat and its diameter was constant. Similarly, Bilir, Ucar, and Oteyaka (2018) also used a single size with a nozzle diameter of 9.5 mm and a solid ratio of 2.5%. So, these values could not be used for full-scale facilities and could not operate at solid rates of up to 40% with high capacity. In this large-scale study, high impact velocities and high air suctions were aimed with hemispherical nozzles of six different diameters. Thus, high CR was aimed for industrial processes. For this reason, optimization attempts were made for 10%, 20% and 30% values with higher solids rates. A similar study was carried out by grinding the coal with 60% solid using by IsaMill, d_{80}: 20–40 µm, to obtain ultrapure coal. Afterwards, enrichment with Jameson cell was applied and high quality charcoal was obtained at 1% wt% ash (Wibberley and Osborne, 2015).

The CR and ash ratios of concentrates taken between 0–3 min, 3–7 min, and 0–7 min were evaluated for the JC (Table 5). The 10% solid/water ratio and nozzle diameter: 7 mm were kept constant. The ash values of the concentrates obtained between 0 and 3 min in flotation are shown in

Table 3. Average CR% and variance values of preliminary tests for reagents.

Collectors	X̄	S^2	Frothers	X̄	S^2
Diesel oil	**91.62**	**1.83**	Pine oil	91.62	1.83
Kerosene	91.59	8.90	MIBC	**94.14**	**0.11**

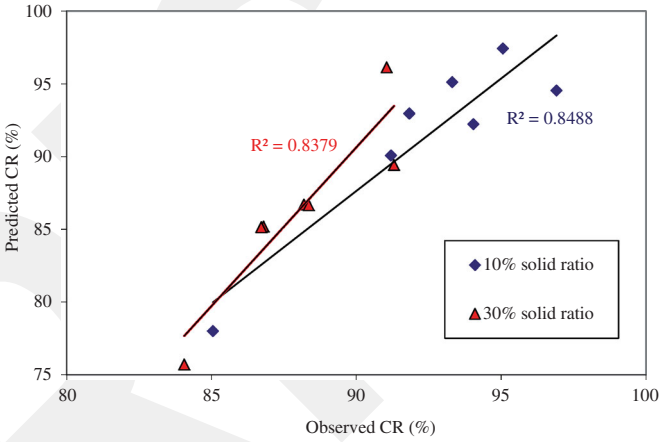

Figure 5. Observed and predicted CR% values of solid/water ratios for 10% and 30% solid ratios.

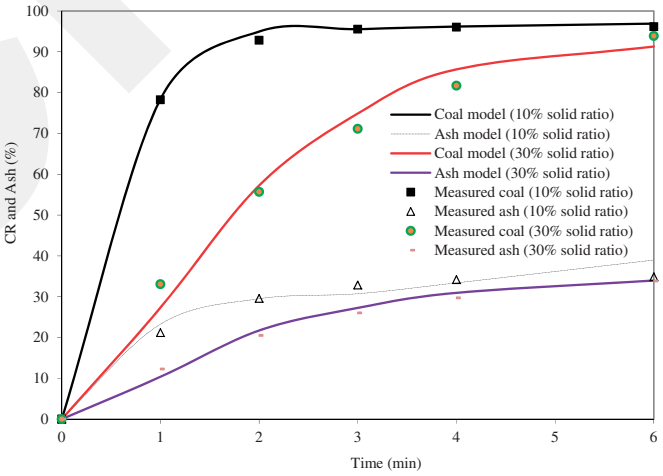

Figure 6. The modified first-order kinetic models used for the determination of optimum test parameters for 10% and 30% solid ratios.

Table 4. Yates test results for 10% solid/water ratio (S: significant, N: not significant).

	CR (%)	1[a]	2[a]	TE[b]	(TE)2/23	DF[c]	FCal[d]	Table value	Decision	X1	X2	X3	Predicted values (%)
	75.45	167.28	355.65	722.85	65,314.02	1				−1	−1	−1	
a	91.83	188.37	367.2	−9.11	10.37	1	3.42	5.32	N	1	−1	−1	92.96
b	93.31	190.95	−18.13	−6.39	5.10	1	1.6826	5.32	N	−1	1	−1	95.12
ab	95.06	176.25	9.02	−17.91	40.10	1	13.218	5.32	S	1	1	−1	97.43
c	**96.91**	−16.38	−21.09	−11.55	16.68	1	5.4973	5.32	S	−1	−1	1	94.54
ac	94.04	−1.75	14.7	−27.15	92.14	1	30.376	5.32	S	1	−1	1	92.23
bc	91.20	2.87	−14.63	−35.79	160.12	1	52.785	5.32	S	−1	1	1	90.07
abc	85.05	6.15	−3.28	−11.35	16.10	1	5.3086	5.32	N	1	1	1	78.81

[a]Yates calculations ($n = 3$), [b]Total effect, [c]Degrees of freedom, [d]$[(TE)^2/2^3]/(DF*\text{Standard error}^2)$.

Table 5. Box Behnken test design with the observed results.

Order	X_1	X_2	X_3	Ash% (0–3 min)	Ash% (3–7 min)	CR% (0–3 min)	CR% (3–7 min)	CR% (0–7 min)	Ash% (0–7 min)
1	2,000	100	50	27.61	52.36	76.10	10.14	86.23	31.77
2	4,000	100	50	17.03	34.36	60.57	34.58	95.16	24.29
3	2,000	300	50	22.29	26.87	40.35	36.13	76.48	13.53
4	4,000	300	50	14.25	39.45	79.11	18.22	97.34	20.45
5	2,000	200	40	15.91	17.54	52.53	21.32	73.85	16.38
6	4,000	200	40	13.05	16.91	57.67	25.11	82.78	14.25
7	2,000	200	60	16.59	26.29	54.08	26.44	80.52	20.04
8	4,000	200	60	10.03	23.07	55.70	27.03	82.74	14.75
9	3,000	100	40	12.46	18.93	53.18	35.47	88.65	15.16
10	3,000	300	40	10.20	19.61	43.01	31.56	74.57	14.43
11	3,000	100	60	11.23	16.87	46.37	30.04	76.42	13.53
12	3,000	300	60	13.33	19.71	59.55	34.28	93.83	15.77
13	3,000	200	50	9.86	15.39	58.73	37.38	96.12	12.09
14	3,000	200	50	21.71	29.63	30.99	39.79	70.79	26.36
15	3,000	200	50	20.08	24.82	46.96	41.97	88.93	22.38

Figure 7(a). As the amount of collector was increased, the ash values of the concentrate were decreased. When the collector amount was increased from 2,000 g/ton to 4,000 g/ton, it was observed that there was a decrease of about 15–20% in the concentrate ash ratio. MIBC did not cause a significant change in the ash values of the floated coals in the first 3 min. As the MIBC ratio increased, the concentration of ash in the concentrate decreased slightly. The synergistic effect of MIBC and diesel was positive. It was clear that the ash contents of the concentrates obtained in the test where the downcomer (DC) depth was 50 cm were at the highest level. However, the ash ratios were low in the experiments performed at 40 and 60 cm downcomer plunge depths (Figure 7(b)). After 3 min, it was seen that the amount of floating coal decreased and the collector floated the impurities as well (Figure 7(c)). The ash ratios of floating coal between 3 and 7 min were similar to the ash ratios of the floating coal between 0 and 3 min according to the downcomer length (Figure 7(d)). The ash ratios were the highest at 50 cm of downcomer plunge depth. The reduction in the proportion of MIBC caused an increase in the ash contents of concentrates. From Figure 7(e), it was concluded that the total CR of concentrates increased in proportion to the amount of diesel oil. A decrease of 200 g/ton of MIBC caused a decline of 5–8% in CRs. Figure 7(f) showed that the CR values increased in direct proportion to the downcomer plunge depth. As the diesel oil amount and the downcomer depth increased, total CRs increased. While the downcomer plunge was short, the CR values decreased as the amount of MIBC increased. However, in tests where the downcomer plunge depth was 60 cm, CRs above 90% could be obtained by increasing the MIBC ratio (Figure 7(g)). When the ash content of coal concentrates obtained between 0 and 7 min was taken into consideration, it was observed that the increase in the ratio of MIBC decreased the ash ratio when the collector ratio was low (Figure 7(h)). The other results can be seen in Figure 7(a,c), similarly. It was determined that MIBC and diesel oil played complementary roles in the tests. In ANOVA analysis equations were formed by using quadratic models. As a result of Box Behnken test design, 3,000 g/ton of diesel oil, 300 g/ton of MIBC and 50 cm of downcomer plunge depth were selected as optimum parameters. In subsequent experiments, the effect of circular nozzle diameters was investigated. Regression correlations for ash values between 0 and 3 min, ash values between 3 and 7 min, CR values between 0 and 3 min, CR values between 3 and 7 min, CR values between 0and 7 min and ash values between 0 and 7 min were 71.5%, 85%, 77%, 97%, 63% and 60%, respectively. Following equations were obtained for total CR% (Equation (7)) and AR% (Equation (8)) of concentrated coals (for 0–7 min). CR% and AR% values for different times were determined to demonstrate the nozzle diameter effects for flotation efficiency.

The CR% values were consistent with the curve created using the first-order kinetic model. The calculated values for different nozzle diameters according to the kinetic model were given in Table 6. The best selectivity index value (SI = k_{coal}/k_{ash}) was calculated as 2.40 for 5 mm nozzle diameter. The materials obtained during flotation in all nozzle diameters increased sharply in the first 2 min and then the floatability speeds decreased. In the next 2 min, the amount of material floated with a 7 mm diameter nozzle was around 15%. This value is approximately 10% for the 9 mm diameter nozzle and 5% for the higher diameter nozzles (Figure 8).

Especially, the efficiency between 3 and 7 min for recovery (%) is very consistent experimental results for ANOVA, statistically. The Model *F*-value of 16.81 shows it is significant. There is only a 0.31% chance that an *F*-value this large could occur due to noise. *p*-Values less than 0.05 mean model terms are notable. In this purpose; AB, A^2, B^2 are significant terms. Values greater than 0.10 designate terms are not remarkable. The Lack of Fit *F*-value of 1.47 implies it has no pure error. There is a 42.91% possibility that non-significant lack of fit is good for an acceptable analysis.

$$Y_1 = 14.03 + 0.01X_1 - 0.63X_2 + 4.47X_3 + 0.00002.9825e - X_1X_2 - 0.01X_1X_3 + 0.01X_2X_3 + 6.375e - 8{X_1}^2 + 0.34e - 3{X_2}^2 - 0.05{X_3}^2 \quad (7)$$

$$Y_2 = -84.59 - 0.02X_1 - 0.18X_2 + 5.99X_3 + 3.6e - 5X_1X_2 - 7.9e - 5\ X_1X_3 + 0.70e - 3X_2X_3 + 1.93e\ 6{X_1}^2 + 3.01e - 5{X_2}^2 - 0.06{X_3}^2 \quad (8)$$

The velocities of flow rates were calculated using V = Q/A. Where V: flow speed (m/s), Q: flow capacity (m^3/s) and A: area of section diameter (m^2). The velocities of water coming out of nozzles with diameters of 5, 7, 9, 11,

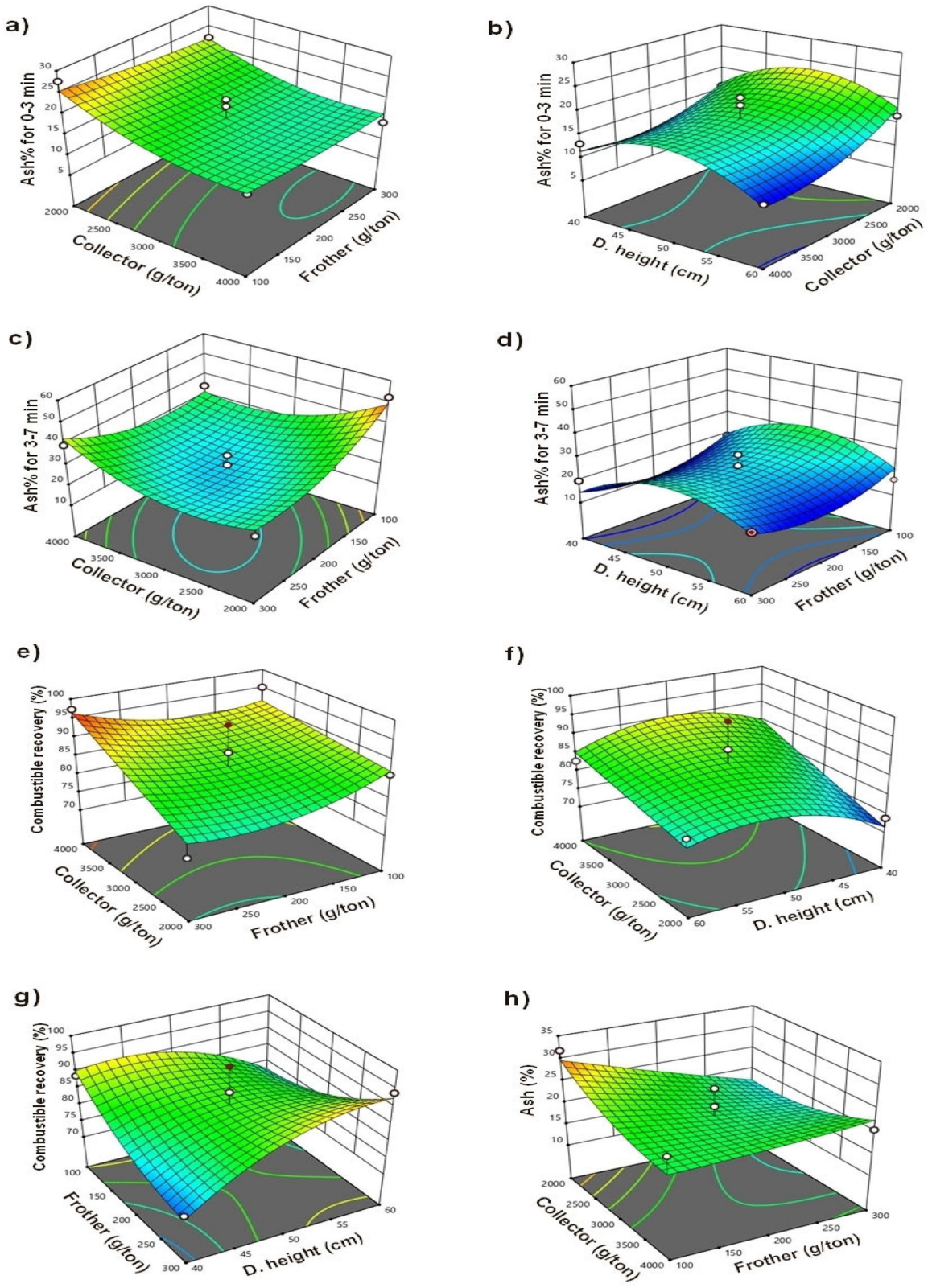

Figure 7. Effective response surface analysis results according to design of experiments.

and 13 mm were determined as 21.22, 10.83, 6.55, 4.38, 3.14 m/sec, respectively. The kinetic models for different nozzle diameters depend on CR% can be seen in Figure 8.

The use of low-diameter nozzles created a water-jet effect in the downcomer and increased the water-particle-air interaction leading the effective coal recovery. The decreases in CRs and ARs show that more flotation time is required at higher nozzle diameters. The effects of velocities were also observed in AR% values (Figure 9). In comparison with the classical Denver flotation, a greater amount of material was floated by JC.

Sahbaz, Ucar, and Oteyaka (2019) stated that downcomer outlet diameter was one of the most suitable solutions to

Table 6. Modified first-order kinetic model parameters for different nozzle diameters.

d (mm)	CR_∞	k_{coal}	R^2	Std. dev.	SI
5	99.77	1.20	0.96	3.67	2.40
7	83.33	1.08	0.94	4.44	1.29
9	73.19	1.13	0.88	5.50	1.59
11	75.61	1.03	0.94	4.42	1.94
13	76.30	0.97	0.98	2.86	2.02

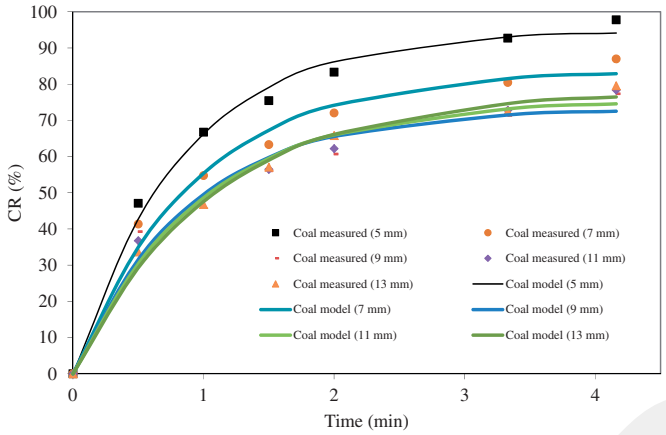

Figure 8. The kinetic models for different nozzle diameters depend on CR%.

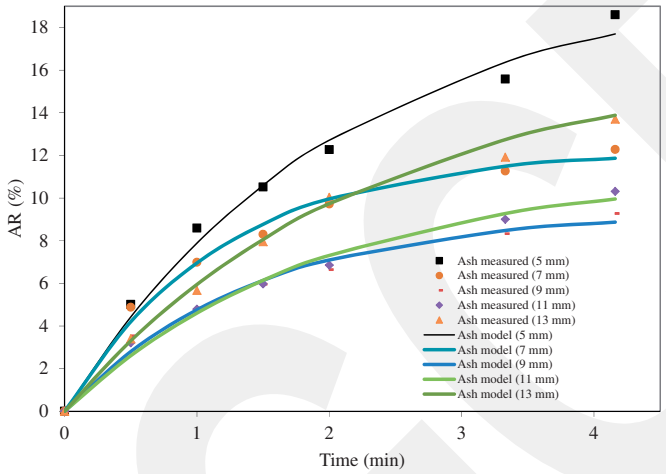

Figure 9. The kinetic models for different nozzle diameters depend on AR%.

reduce turbulence, and consequently, decreasing turbulence caused an increase in maximum floatable particle sizes. From the innovative test results of this study, it can be said that the increase in the nozzle diameter decreases the turbulence and increases the floating particle size. Although it causes a more turbulent flow, experiments performed with a 5 mm nozzle diameter resulted in a finer clean coal recovery consisting of free coal particles.

4. Conclusions

The optimum collector and frother for recovery of HCT using Yates test technique were determined as diesel oil and MIBC, respectively. Then, JC tests were performed using Box Behnken test design for new type of circular nozzles. The use of lower-diameter circular nozzles created a venturi effect of air current and a negative vacuum leading to a reduction in fluid pressure and an increase in fluid velocity. By using circular nozzle of 5 mm, a higher amount of cleaner coal was obtained with JC compared to conventional Denver flotation cell. This indicated the increased CC. The average CRs (%) were over 95% as a good effect of the cell design. The average calorific values of the concentrates were 6,550 ± 100 kcal/kg. The fixed Carbon ratio was found to be 54.55% according to ASTM standards (Table 7). This study showed that the clean coal with high recovery ratios and low ash rates could be separated from the HCT using proper nozzle diameter. Therefore, a qualified concentrate with suitable CC could be recycled. The product can be used for coke and semi-coke processes for blast furnace industry as a qualified fuel source and this process can provide prevention of air pollution with a low sulfur content (0.38%).

Table 7. Analysis results of the concentrate.

Contents	%
Moisture	1.36
Ash	17.81
Volatile matter	23.15
Total sulfur	0.38
Calorific value (kcal/kg) ± 100	6,550
Fixed carbon	54.55

Disclosure statement

No potential competing interest was reported by the author(s).

Funding

This research was supported by Cukurova University [Project Code: MMF2009YL47].

ORCID

Soner Top http://orcid.org/0000-0003-3486-4184
Mahmut Altiner http://orcid.org/0000-0002-7428-5999

References

Ahmed, N., and G. J. Jameson. 1985. The effect of bubble size on the rate of flotation of fine particles. *International Journal of Mineral Processing* 14 (3):195–215. doi:10.1016/0301-7516(85)90003-1.

Asghar, A., H. Ahmad, and F. Behnam. 2015. Investigating the first-order flotation kinetics models for Sarcheshmeh copper sulfide ore. *International Journal of Mining Science and Technology* 25 (5):849–54. doi:10.1016/j.ijmst.2015.07.022.

Barraza, J., J. Guerrero, and J. Pineres. 2013. Flotation of a refuse tailing fine coal slurry. *Fuel Processing Technology* 106:498–500. doi:10.1016/j.fuproc.2012.09.018.

Bilir, K., A. Ucar, and B. Oteyaka. 2018. Comparison of Jameson cell and jet diffuser flotation column. *Physicochemical Problems of Mineral Processing* 54: 174–81. doi:10.5277/ppmp1836.

Coker, A. K. 1991. Understanding the basics of packed-column design. *Chemical Engineering Progress* 1991: 93–9.

Dey, S., G. M. Paul, and S. Pani. 2013. Flotation behaviour of weathered coal in mechanical and column flotation cell. *Powder Technology* 246:689–94. doi:10.1016/j.powtec.2013.06.015.

Gürsoy, Y. H., and B. Öteyaka. 2015. The effects of aır-to-pulp ratıo and bıas factor on flotatıon of complex Cu-Zn sulphıde ore ın the Jameson cell. *Physicochemical Problems of Mineral Processing* 51 (2): 511–9. doi:10.5277/ppmp150212.

Hacifazlioglu, H., and I. Toroglu. 2007. Optimization of design and operating parameters in a pilot scale Jameson cell for slime coal cleaning. *Fuel Processing Technology* 88 (7):731–6. doi:10.1016/j.fuproc.2007.03.003.

Harbort, G. J., S. De Bono, D. Carr, and V. Lawson. 2003. Jameson cell fundamentals—A revised perspective. *Minerals Engineering* 16 (11): 1091–101. doi:10.1016/j.mineng.2003.06.008.

Li, B., D. Tao, Z. Ou, and J. Liu. 2003. Cyclo-microbubble column flotation of fine coal. *Separation Science and Technology* 38 (5):1125–40. doi:10.1081/SS-120018127.

Li, Y., J. Li, P. Chen, J. Chen, L. Shen, X. Zhu, and G. Cheng. 2019. The effect of ultra-fine coal on the flotation behavior of silica in subbituminous coal reverse flotation. *Powder Technology* 342:457–63. doi:10.1016/j.powtec.2018.10.014.

Mazahernasab, R., and R. Ahmadi. 2016. Determination of bubble size distribution in a laboratory mechanical flotation cell by a laser diffraction technique. *Physicochemical Problems of Mineral Processing* 52 (2):690–702. DOI:10.5277/ppmp160214.

Meshram, P., B. K. Purohit, M. K. Sinha, S. K. Sahu, and B. D. Pandey. 2015. Demineralization of low grade coal – A review. *Renewable and Sustainable Energy Reviews* 41 (1):745–61. doi:10.1016/j.rser.2014.08.072.

Miettinen, T., J. Ralston, and D. Fornasiero. 2010. The limits of fine particle flotation. *Minerals Engineering* 23 (5):420–37. doi:10.1016/j.mineng.2009.12.006.

Mohanty, M. K., and R. Q. Honaker. 1999. Performance optimization of Jameson flotation technology for fine coal cleaning. *Minerals Engineering* 12 (4):367–81. doi:10.1016/S0892-6875(99)00017-5.

Ni, C., X. Bu, W. Xia, Y. Peng, and G. Xie. 2018. Effect of slimes on the flotation recovery and kinetics of coal particles. *Fuel* 220:159–66. doi:10.1016/j.fuel.2018.02.003.

Ramudzwagi, M., N. Tshiongo-Makgwe, and W. Nheta. 2020. Recent developments in beneficiation of fine and ultra-fine coal – Review paper. *Journal of Cleaner Production* 276:122693–11. doi:10.1016/j.jclepro.2020.122693.

Sahbaz, O., A. Ucar, and B. Oteyaka. 2019. Downcomer modification in the Jameson cell and its effects on coarse particle flotation. *Particulate Science and Technology* 37 (4):514–9. doi:10.1080/02726351.2017.1372826.

Sahbaz, O., and M. K. Demir. 2020. Effects of frothers and particle size on the flotation kinetics of the Jameson cell. *Physicochemical Problems of Mineral Processing* 56 (5):829–38. doi:10.37190/ppmp/125917.

Vapur, H., O. Bayat, and M. Ucurum. 2010. Coal flotation optimization using modified flotation parameters and combustible recovery in a Jameson cell. *Energy Conversion and Management* 51 (10):1891–7. doi:10.1016/j.enconman.2010.02.019.

Wang, G., B. Xuetao, W. Changning, L. Weng, L. Ke, and K. Ali. 2018. Recent advances in the beneficiation of ultrafine coal particles. *Fuel Processing Technology* 178:104–25. doi:10.1016/j.fuproc.2018.04.035.

Wang, J., and L. Wang. 2018. Improving column flotation of oxidized or ultrafine coal particles by changing the flow pattern of air supply. *Minerals Engineering* 124:98–102. doi:10.1016/j.mineng.2018.05.018.

Wibberley, L. J., and D. Osborne. 2015. Premium coal fuels with advanced coal beneficiation. Clearwater Clean Coal Conference, Clearwater, FL.

Wills, B. A., and J. Finch. 2015. *Wills' mineral processing technology: An introduction to the practical aspects of ore treatment and mineral recovery*. 8th ed. Waltham (MA): Butterworth-Heinemann.

Xing, Y., X. Gui, Y. Cao, D. Wang, and H. Zhang. 2017. Clean low-rank-coal purification technique combining cyclonic-static microbubble flotation column with collector emulsification. *Journal of Cleaner Production* 153:657–72. doi:10.1016/j.jclepro.2016.11.057.

Yan, Y., and G. J. Jameson. 2004. Application of the Jameson cell technology for algae and phosphorus removal from maturation ponds. *International Journal of Mineral Processing* 73 (1):23–8. doi:10.1016/j.minpro.2003.07.002.

You, X., L. Li, J. Liu, L. Wu, M. He, and X. Lyu. 2017. Investigation of particle collection and flotation kinetics within the Jameson cell downcomer. *Powder Technology* 310:221–7. doi:10.1016/j.powtec.2017.01.002.

Zhu, H., A. L. Valdivieso, J. Zhu, S. Song, F. Min, and M. A. C. Arroyo. 2018. A study of bubble size evolution in Jameson flotation cell. *Chemical Engineering Research and Design* 137:461–6. doi:10.1016/j.cherd.2018.08.005.